

Electromagnetic response of a metamaterial with field-gradient-induced transparency

Yasuhiro Tamayama,* Toshihiro Nakanishi, Yasuhiro Wakasa,
Tetsuo Kanazawa, Kazuhiko Sugiyama, and Masao Kitano

Department of Electronic Science and Engineering, Kyoto University, Kyoto 615-8510, Japan

(Dated: November 13, 2018)

We investigate a dynamically controllable electromagnetically induced transparency-like metamaterial. The unit structure of the metamaterial consists of a low-quality-factor resonator and a high-quality-factor resonator. The field gradient of the incident electromagnetic wave in the transverse direction induces coupling between these two types of resonators and causes a transparency phenomenon. We present the simulation and experimental results for the dynamic control of the electromagnetic response.

PACS numbers: 78.67.Pt, 42.25.Bs, 78.20.Ci

I. INTRODUCTION

A number of studies have focused on controlling the propagation of electromagnetic waves using metamaterials that consist of periodically or randomly arranged artificial subwavelength structures. Metamaterials can even be used to obtain extraordinary media that do not occur in nature, such as media with a negative refractive index.¹ Metamaterials have been applied to demonstrate various phenomena, such as subwavelength imaging,^{2,3} cloaking,^{4,5} and no-reflection propagation.^{6,7}

On the other hand, electromagnetically induced transparency (EIT) has attracted considerable attention in recent years as a means by which to achieve extremely low group velocity propagation of electromagnetic waves.^{8,9} Electromagnetically induced transparency is a quantum phenomenon that arises in three-state Λ -type atoms interacting with electromagnetic fields, and causes the suppression of the absorption of incident electromagnetic waves in a narrow frequency range. Based on the Kramers-Kronig relations,¹⁰ steep dispersion, or low group velocity, can be achieved in the frequency range. In fact, a group velocity of $17 \text{ m/s} \sim 10^{-7} c_0$ (where c_0 is the speed of light in a vacuum) has been observed using the phenomenon.¹¹

Since a somewhat complicated arrangement is necessary in order to achieve EIT, a number of studies have focused on mimicking the effect in classical systems, such as optical resonators,¹²⁻¹⁵ waveguides,¹⁶ and metamaterials.¹⁷⁻²⁴ However, few studies have focused on the dynamic control of the transmission spectrum in classical EIT-like systems. In the present study, we investigate an EIT-like metamaterial having properties that can be controlled dynamically.

First, we describe the structure of the EIT-like metamaterial. The unit cell of the metamaterial consists of a low-quality-factor (Q) resonator and a high- Q resonator. The field gradient of the incident electromagnetic wave in the transverse direction induces coupling between these two types of resonators and causes a transparency phenomenon in the metamaterial. Then, we describe how to control the electromagnetic response of the metama-

terial. We present the experimental results for the dynamic control of the transparent frequency using variable capacitance diodes and the simulation results for the dynamic control of the frequency width of the transparency window. Although the experiment is performed in the microwave region, it may be possible to perform similar experiments in the terahertz and optical regions.

II. THEORY

Figure 1(a) shows a capacitively loaded strip metamaterial.²⁵ The metamaterial can be regarded as series inductor-capacitor resonant circuits that consist of metal strips in the x direction and gaps between the neighboring structures in the x direction. When a plane electromagnetic wave is incident on the metamaterial, as shown in Fig. 1(a), the metamaterial behaves as a Lorentz-type dielectric medium because currents are induced in the x direction by the incident electric field and the electric dipoles are excited.

We now consider the metamaterial shown in Fig. 1(b). Each capacitively loaded strip is connected to the neighboring structures in the y direction. The metamaterial shown in Fig. 1(b) includes two types of series inductor-capacitor resonant circuits. One consists of a metal strip in the x direction and a gap between the neighboring structures in the x direction, which is the same as the resonant circuit in the capacitively loaded strips. The other consists of a metal strip in the y direction and a gap between the neighboring structures in the x direction. (The numerically calculated current and electric field distributions in the metamaterial are shown in Fig. 4 and can be used to determine the portions of each structure that act as inductors and capacitors.) The former resonant circuit is referred to as resonator 1, and the latter resonant circuit as resonator 2. These two types of resonators are magnetically coupled to each other. The x -polarized incident electric field can directly excite only resonator 1. Resonator 2 cannot be excited directly because the direction of current flow in resonator 2 is perpendicular to the direction of the incident electric field.

Magnetic coupling occurs between the two types of

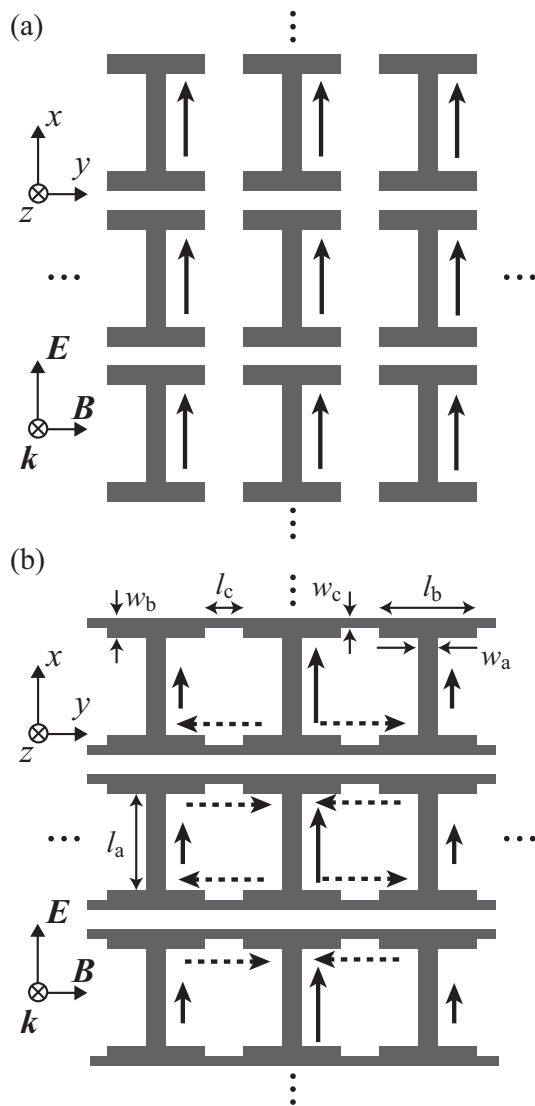


FIG. 1: (a) Metal structure of the capacitively loaded strips and (b) the field-gradient-induced-transparency metamaterial. The solid (dashed) arrows represent the current in resonator 1 (resonator 2).

resonators when the field gradient of the incident electromagnetic fields exists. When the x component of the electric field has a gradient in the y direction, the induced current in resonator 1 becomes y dependent. The difference between adjacent currents creates a magnetic flux through the loop of resonator 2 and induces anti-parallel currents via the electromotive force. When the incident electromagnetic wave is a plane wave, this coupling vanishes due to the uniformity in the y direction of the currents in resonator 1. Thus, only resonator 1 can be excited. In this case, the metamaterial behaves as a Lorentz-type medium, as in the case of the capacitively loaded strips.

The resonance mode in resonator 1 is electric dipole

resonance whereas that in resonator 2 is weak radiative resonance, i.e., trapped-mode resonance.²⁶ This implies that resonator 2 has a higher Q value than resonator 1. Therefore, this system is similar to the classical model of EIT.²⁷ When the difference between the frequency of the incident electromagnetic wave and the resonance frequency of resonator 2 is large, resonator 2 is excited only slightly and the properties of the metamaterial are determined primarily by resonator 1. Thus, the metamaterial behaves almost as a Lorentz-type dielectric medium. When the frequency of the electromagnetic wave is nearly equal to the resonance frequency of resonator 2, resonator 2 is excited through the coupling with resonator 1. Resonator 2 stores the electromagnetic energy with low loss because its Q value is high. The current in resonator 1 is the sum of the current induced by the incident electromagnetic wave and the current induced by resonator 2. Due to destructive interference between these currents, the current in resonator 1 might vanish, at which point the metamaterial would become transparent. Since the transparency phenomenon is induced by the field gradient of electromagnetic waves, we refer to the metamaterial as a “field-gradient-induced-transparency metamaterial.”

We can tune three parameters in order to control the electromagnetic response of our metamaterial: the resonance frequencies of resonators 1 and 2, and the field gradient in the y direction of the incident electromagnetic wave. The first two parameters determine the center frequency of the absorption line and that of the transparency window, respectively. The third parameter corresponds to the coupling strength between resonators 1 and 2 and determines the frequency width of the transparency window.

III. EXPERIMENT ON DYNAMIC CONTROL OF TRANSPARENT FREQUENCY

We fabricated the metamaterial shown in Fig. 2 using printed circuit board technology. The thicknesses of the copper layer and the FR-4 substrate (relative permittivity: 4.5) of the printed circuit board were $35 \mu\text{m}$ and 1.6 mm , respectively. We used a structure that was slightly different from that shown in Fig. 1(b) to adjust the resonance frequencies of resonators 1 and 2. We introduced variable capacitance diodes (Infineon BB857) for dynamic control of the resonance frequency of resonator 2. Their capacitances were tuned by applying a direct current reverse bias voltage.²⁸

We measured the transmissivity and the group delay of the fabricated metamaterial using a network analyzer. A layer of the metamaterial was placed in a rectangular waveguide, the cross-sectional dimensions in the x and y directions of which were 34.0 mm (height) and 72.1 mm (width), respectively. The measurement was performed in the frequency region in which only the TE_{10} mode²⁹ can propagate. The waveguide walls parallel to the yz

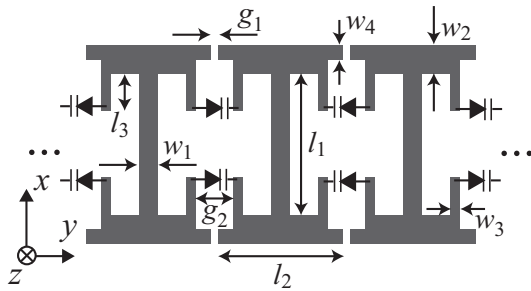


FIG. 2: Schematic of the metamaterial used for the experimental demonstration. The geometrical parameters are $l_1 = 29.1$ mm, $l_2 = 11.8$ mm, $l_3 = 5.0$ mm, $w_1 = 3.0$ mm, $w_2 = 2.0$ mm, $w_3 = 0.5$ mm, $w_4 = 1.0$ mm, $g_1 = 0.4$ mm, and $g_2 = 1.0$ mm.

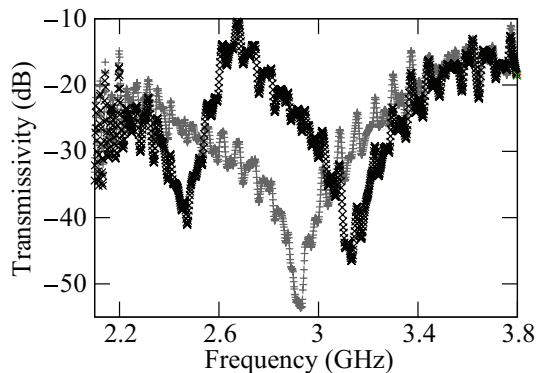


FIG. 3: Transmission spectra of the metamaterial shown in Fig. 2 with diodes (black) and without diodes (gray). The reverse bias voltage on the diodes is zero.

plane are equivalent to periodic boundaries because the electromagnetic fields are uniform in the x direction. The width of the waveguide determines the field gradient of the electromagnetic waves in the y direction.

Figure 3 shows the measured transmission spectra for the cases in which variable capacitance diodes are connected (black) and not connected (gray). These two cases correspond to the field-gradient-induced-transparency metamaterial and the capacitively loaded strips. In the latter case, a simple absorption spectrum is observed, as in the case of a Lorentz-type medium. In the former case, a transmission window is seen in the absorption band, as in the case of an EIT-like medium. Figure 4(a) shows the numerically calculated current and electric field distributions at the resonance frequency of the capacitively loaded strips shown in Fig. 1(a). Figure 4(b) shows the distributions of resonator 2 in the field-gradient-induced-transparency metamaterial shown in Fig. 1(b). We used the COMSOL Multiphysics finite element solver. A section of the metal at the center of the I-shaped structure was replaced with a piece of dielectric medium so that we

can tune the resonance frequency of resonator 1 to that of resonator 2. The current distribution and the electric field distribution enable us to locate the portions of the structure that act as inductors and capacitors. The metal strip in the vertical direction (horizontal direction) constitutes the inductor for resonator 1 (resonator 2), and the gap between the neighboring I-shaped structures in the vertical direction constitutes the capacitor for both resonators. It is confirmed that the electric dipole resonance arises at the resonance frequency in the capacitively loaded strips and that the trapped-mode resonance arises at the resonance frequency of resonator 2 in the field-gradient-induced-transparency metamaterial. Note that no significant current flows in the vertical direction in the case of Fig. 4(b).

Figure 5 shows the measured transmissivity and the group delay of our metamaterial as a function of frequency for three different reverse bias voltages on the variable capacitance diodes. The center frequency of the transparency window (low group-velocity band) is increased by increasing the reverse bias voltage, i.e., by decreasing the capacitance of the diodes.

Next, we present a quantitative analysis of our metamaterial. The charges q_1 and q_2 in resonators 1 and 2, respectively, are assumed to satisfy the following equations:

$$\frac{d^2 q_1}{dt^2} + (2\pi\gamma_1) \frac{dq_1}{dt} + (2\pi f_1)^2 q_1 - (2\pi\kappa)^2 q_2 = \alpha' \tilde{E} e^{-i2\pi f t} + \text{c.c.}, \quad (1)$$

$$\frac{d^2 q_2}{dt^2} + (2\pi\gamma_2) \frac{dq_2}{dt} + (2\pi f_2)^2 q_2 - (2\pi\kappa)^2 q_1 = 0, \quad (2)$$

where f is the frequency of the incident field, f_1 (f_2) is the resonance frequency of resonator 1 (2), γ_1 (γ_2) is the loss in resonator 1 (2), κ is the coupling factor between resonators 1 and 2, \tilde{E} is the complex amplitude of the incident electric field, α' is a constant, and c.c. stands for the complex conjugate of the preceding term.²⁷ The electric susceptibility of the metamaterial is given as

$$\chi_e(f) = \frac{-\alpha(f^2 + i\gamma_2 f - f_2^2)}{(f^2 + i\gamma_1 f - f_1^2)(f^2 + i\gamma_2 f - f_2^2) - \kappa^4} \left(\propto \frac{\tilde{q}_1}{\tilde{E}} \right), \quad (3)$$

where $q_1 = \tilde{q}_1 e^{-i2\pi f t} + \text{c.c.}$ and α is a constant. Assuming that $f_1 \approx f_2$ and $\gamma_1 \gg \gamma_2$, we find that the transmittance at f_2 , which is the transparent frequency, decreases with decreasing κ , and the bandwidth of the transparency window can be approximated as κ^2/f_2 . The group velocity at f_2 is found to decrease with decreasing κ until κ^2/f_2 reaches approximately $\sqrt{\gamma_1 \gamma_2}$.¹⁷ Therefore, we can consider the minimum bandwidth of the transparency window to be $\sqrt{\gamma_1 \gamma_2}$. The transmissivity t of the metamaterial is written as follows:³⁰

$$t = \frac{4Z_1 Z_2}{[(Z_2 + Z_1)^2 e^{-ik_2 d} - (Z_2 - Z_1)^2 e^{ik_2 d}] e^{ik_1 d}}, \quad (4)$$

where $k_1 = (2\pi f/c_0) \sqrt{1 - [c_0/(2wf)]^2}$, $k_2 = (2\pi f/c_0) \sqrt{1 + \chi_e - [c_0/(2wf)]^2}$, $Z_1 = 2\pi f \mu_0/k_1$, $Z_2 =$

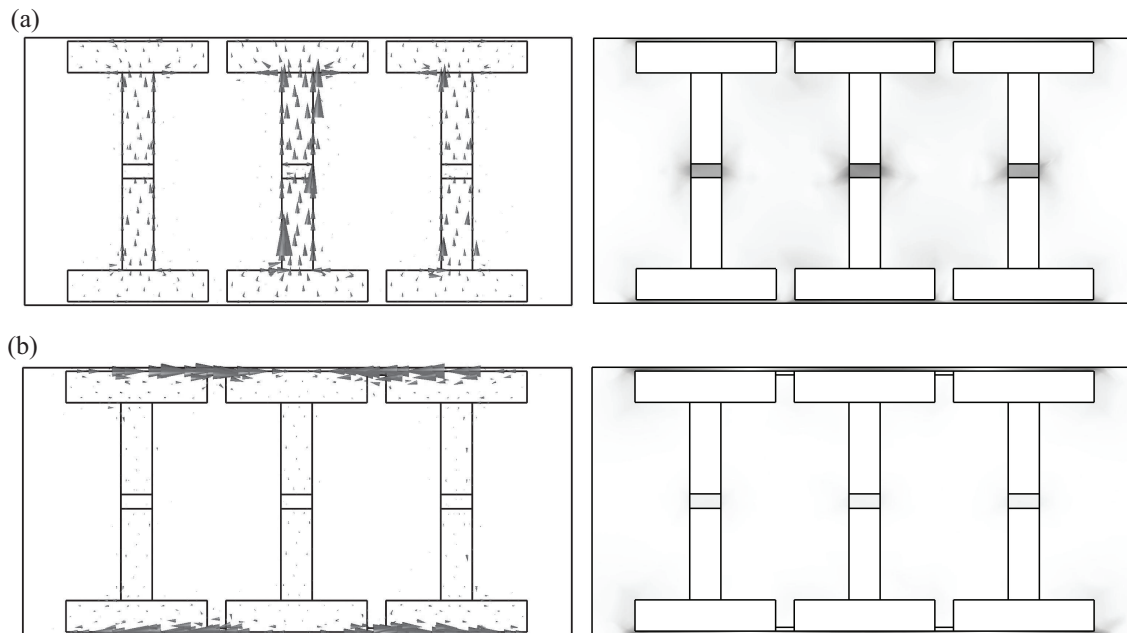


FIG. 4: Current distributions (left panel) and electric field distributions (right panel) in (a) the capacitively loaded strips [Fig. 1(a)] at the resonance frequency f_1 of the electric dipole resonance and in (b) the field-gradient-induced-transparency metamaterial [Fig. 1(b)] at the resonance frequency f_2 of resonator 2. In the right-hand panels, black (white) corresponds to a large (small) electric field. The outer boxes represent the waveguide walls (perfect electric conductors). A section of the metal at the center of the I-shaped structure is replaced by a piece of dielectric medium in order to tune f_1 and f_2 . The relative field strengths in (a) and (b) are not scaled.

$2\pi f \mu_0 / k_2$,²⁹ w is the waveguide width, μ_0 is the permeability of the vacuum, and d is the thickness of the metamaterial. We adopt $d = 1.7$ mm from the physical thickness of the metamaterial. It is difficult to define the thickness of a single-layer metamaterial. However, in the present case, the change in d has little effect on the following fitting results. We compare t with the measured transmission spectra.

The fitted curves of $|t|$, and the fitting parameters are shown in the upper row of Fig. 5. Here, we adopt the values of $f_1 = 2.93$ GHz and $\gamma_1 = 0.20$ GHz derived from the measured transmissivity and group delay (not shown) of our metamaterial without the diodes and assume that f_2 , γ_2 , κ , and α are fitting parameters. Although the measured and fitted transmissivities are slightly different in the lower-frequency region, they agree rather well with each other. The group delay $\{d[\arg(t)]/df\}/2\pi$ calculated using the obtained fitting parameters is shown in the lower row of Fig. 5. The measured group delay is in good agreement with the calculated value.

Based on the above results, the condition whereby $\kappa^2/f_2 > \gamma_1 > \gamma_2$ is satisfied. This implies that low- Q resonator 1 is strongly coupled to high- Q resonator 2. In addition, f_2/γ_2 is found to increase with the reverse bias voltage. This is because the resistance of the variable capacitance diode, which determines the loss of resonator 2, decreases with increasing reverse bias voltage. The value f_2/κ is independent of the reverse bias voltage, i.e., the

coupling strength between resonators 1 and 2 does not depend on the resonance frequency of resonator 2. A possible reason for the slight difference between the measured and fitted values is that we used one layer of the metamaterial in the experiment whereas in the theoretical model, we assumed a homogeneous medium. The oblique propagation in the waveguide²⁹ may also have to be considered.

In order to confirm the Q values of the two types of resonators, we performed COMSOL simulations and found that $Q_1 = f_1/\gamma_1 = 9.1$ and $Q_2 = f_2/\gamma_2 = 71$. The dielectric loss tangent of the substrate was assumed to be 0.02. The Q values calculated from the fitting result for the reverse bias voltage of 30 V were $Q_1 = 15$ and $Q_2 = 83$. The experimental values are slightly larger than the simulated values for both types of resonators. This might be because an actual value of the dielectric loss tangent of the substrate was smaller than 0.02. The ratio Q_2/Q_1 for the experiment might be smaller than that for the simulation because of the resistance of the diodes.

IV. SIMULATION OF DYNAMIC CONTROL OF COUPLING STRENGTH

We performed numerical simulations using COMSOL Multiphysics to confirm that the coupling strength between resonators 1 and 2 depends on the field gradient

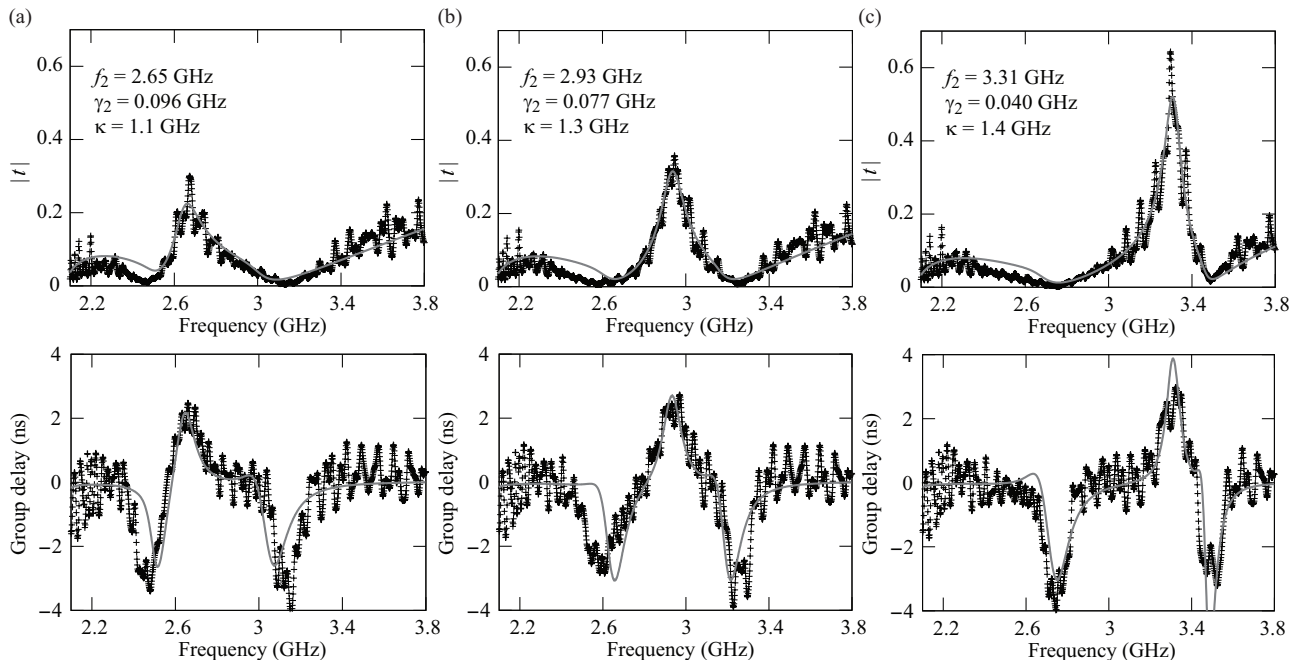


FIG. 5: Transmissivity (upper row) and group delay (lower row) of the fabricated metamaterial as a function of frequency. Black crosses and gray solid curves represent the measured data and the fitting curves, respectively. The reverse bias voltage on the variable capacitance diodes are (a) 0 V, (b) 10.5 V, and (c) 30 V.

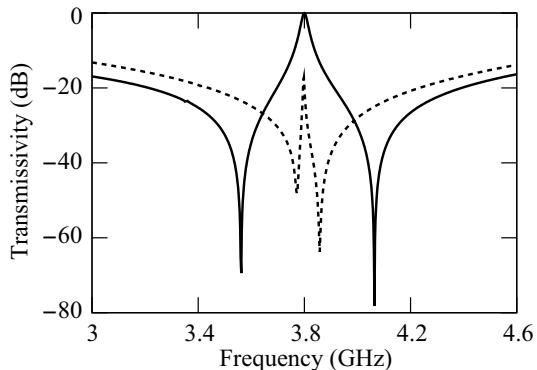


FIG. 6: Dependence of the transmission spectrum on the waveguide width or the field gradient in the y direction of the incident electromagnetic wave. The waveguide width for the dashed curve is 2.2 times larger than that for the solid curve.

in the y direction. We calculated the transmissivity of the metamaterial placed in a rectangular waveguide. We changed the width of the waveguide in order to control the field gradient in the y direction of the incident electromagnetic wave and calculated the transmissivity for several values of the waveguide width.

Figure 6 shows the transmission spectra of the metamaterial shown in Fig.1(b) for the TE_{10} mode. The geometric parameters of the metamaterial were $l_a = 25.1$ mm, $l_b = 18.0$ mm, $l_c = 2.4$ mm, $w_a = 4.0$ mm,

$w_b = 4.0$ mm, and $w_c = 0.5$ mm, and the thickness of the metal was 0.5 mm. The metal pattern was on a dielectric substrate of 0.5 mm in thickness having a relative permittivity of 4.5. In order to tune the resonance frequency of resonator 1 to that of resonator 2, we replaced part of the metal at the center of the I-shaped structure with a piece of dielectric medium, the length and relative permittivity of which were 1.8 mm and 24.5, respectively (see Fig. 4). The dimensions of the cross section of the waveguide in the x and y directions when the solid curve (dashed curve) was obtained were 34.0 mm and 70.0 mm (34.0 mm and 153.7 mm), respectively. We confirmed that the transparency window narrows as the waveguide width increases. In other words, the smaller the field gradient in the y direction of the incident electromagnetic wave, the weaker the coupling strength between resonators 1 and 2.

V. SUMMARY AND DISCUSSION

We investigated a dynamically controllable metamaterial that behaves as an EIT-like medium. The unit structure of the metamaterial is composed of a low- Q resonator (resonator 1) and a high- Q resonator (resonator 2). When a plane electromagnetic wave is incident on the metamaterial, only resonator 1 can be excited. Resonator 1 couples to resonator 2 when the incident electromagnetic wave has a field-gradient in the transverse direction, such as a Gaussian beam. The system is similar to the

classical analog of EIT, and the metamaterial behaves as an EIT-like medium. We described a method by which to control the electromagnetic response of the metamaterial. We experimentally demonstrated dynamic control of the transparent frequency, i.e., the resonance frequency of resonator 2 of the metamaterial, using variable capacitance diodes. The simulations confirmed that the frequency width of the transparency window, or the coupling strength between resonators 1 and 2, can be controlled by the field gradient in the transverse direction of the incident electromagnetic wave.

In our experiment, the ratios of the wavelength to the length of the unit structure in the x and y directions are 2.3 and 6.5, respectively. These ratios are larger than 2, and thus the diffraction can safely be neglected. For normal incidence, in particular, the diffraction does not arise when these ratios are larger than 1. This implies that effective-medium parameters of the metamaterial can be defined. That is, the metamaterial can be regarded as a homogeneous medium. For a larger ratio in the x direction, we could reduce the length of the unit structure in the x direction while preserving the resonance frequencies of resonators 1 and 2 by reducing l_1 and w_1 .

Although we performed our experiment in the microwave region, it is not difficult to conduct similar experiments in higher-frequency regions, such as the terahertz and optical regions. Since the structure of our metamaterial is planar, we can fabricate the metamaterial in the optical region by standard photolithography techniques. We measured the transmission spectrum of the fabricated metamaterial in the waveguide, where the beamwidth of the electromagnetic wave is similar to the wavelength. In the optical region, it is possible to obtain a focus spot size close to the diffraction limit, and hence, it is possible to control the coupling strength between resonators 1 and 2 in free space. We controlled the resonance frequency of resonator 2 by using variable capacitance diodes. The resonance frequency can be controlled by using the photoexcitation of carriers in a semiconductor in the terahertz region³¹ and the phase transitions of liquid crystal³² and vanadium oxide³³ in the optical region.

Field-gradient-induced-transparency metamaterials have numerous applications. The difference between the

capacitively loaded strips shown in Fig.1(a) and our metamaterial shown in Fig.1(b) is whether or not the I-shaped metal structures are connected to neighboring structures. Therefore, we can dynamically switch from a Lorentz-type medium to an EIT-like medium and vice versa by controlling the resistance of the connection using the photoexcitation of carriers³⁴ or Schottky junction.³⁵ This indicates that a dynamic field-gradient-induced-transparency metamaterial could be used as an amplitude modulator. Since the transparency window is narrow and the transparent frequency depends on the inductance and capacitance that form resonator 2, our metamaterial can be used for high-sensitivity sensing. The metamaterial can also be applied to transverse-mode filters and measurements of beamwidth because the transmission spectrum depends on the field gradient in the transverse direction of the incident electromagnetic wave.

Field-gradient-induced-transparency bears a resemblance to nuclear quadrupole resonance. In nuclear quadrupole resonance, the energy level of nuclear spin splits due to the interaction between the electric quadrupole moment of atomic nuclei having a nuclear spin greater than 1/2 and the electric field gradient at the atomic nuclei that is caused by electrons. The splitting width of the energy level increases with the electric field gradient. In field-gradient-induced transparency, the frequency separation between the two dips in the transmission spectrum increases with the field gradient in the transverse direction of the incident electromagnetic waves.

Acknowledgments

This research was supported by a Grant-in-Aid for Scientific Research on Innovative Areas under Grant No.22109004 and the Global COE program “Photonics and Electronics Science and Engineering” at Kyoto University. One of the authors (Y.T.) would like to acknowledge the support from the Japan Society for the Promotion of Science.

* Electronic address: tama@giga.kuee.kyoto-u.ac.jp

¹ R. A. Shelby, D. R. Smith, and S. Schultz, *Science* **292**, 77 (2001).

² A. N. Lagarkov and V. N. Kissel, *Phys. Rev. Lett.* **92**, 077401 (2004).

³ Z. Liu, H. Lee, Y. Xiong, C. Sun, and X. Zhang, *Science* **315**, 1686 (2007).

⁴ D. Schurig, J. J. Mock, B. J. Justice, S. A. Cummer, J. B. Pendry, A. F. Starr, and D. R. Smith, *Science* **314**, 977 (2006).

⁵ R. Liu, C. Ji, J. J. Mock, J. Y. Chin, T. J. Cui, and D. R.

Smith, *Science* **323**, 366 (2009).

⁶ Y. Tamayama, T. Nakanishi, K. Sugiyama, and M. Kitano, *Phys. Rev. B* **73**, 193104 (2006).

⁷ B. Edwards, A. Alù, M. E. Young, M. Silveirinha, and N. Engheta, *Phys. Rev. Lett.* **100**, 033903 (2008).

⁸ S. E. Harris, *Phys. Today* **50**, 36 (1997).

⁹ M. Fleischhauer, A. Imamoglu, and J. P. Marangos, *Rev. Mod. Phys.* **77**, 633 (2005).

¹⁰ B. E. A. Saleh and M. C. Teich, *Fundamentals of Photonics* (Wiley-Interscience, Hoboken, NJ, 2007), 2nd ed.

¹¹ L. V. Hau, S. E. Harris, Z. Dutton, and C. H. Behroozi,

- Nature **397**, 594 (1999).
- ¹² D. D. Smith, H. Chang, K. A. Fuller, A. T. Rosenberger, and R. W. Boyd, Phys. Rev. A **69**, 063804 (2004).
 - ¹³ M. F. Yanik, W. Suh, Z. Wang, and S. Fan, Phys. Rev. Lett. **93**, 233903 (2004).
 - ¹⁴ K. Totsuka, N. Kobayashi, and M. Tomita, Phys. Rev. Lett. **98**, 213904 (2007).
 - ¹⁵ X. Yang, M. Yu, D.-L. Kwong, and C. W. Wong, Phys. Rev. Lett. **102**, 173902 (2009).
 - ¹⁶ H.-C. Liu and A. Yariv, Opt. Express **17**, 11710 (2009).
 - ¹⁷ S. Zhang, D. A. Genov, Y. Wang, M. Liu, and X. Zhang, Phys. Rev. Lett. **101**, 047401 (2008).
 - ¹⁸ N. Papasimakis, V. A. Fedotov, N. I. Zheludev, and S. L. Prosvirnin, Phys. Rev. Lett. **101**, 253903 (2008).
 - ¹⁹ N. Papasimakis, Y. H. Fu, V. A. Fedotov, S. L. Prosvirnin, D. P. Tsai, and N. I. Zheludev, Appl. Phys. Lett. **94**, 211902 (2009).
 - ²⁰ P. Tassin, L. Zhang, T. Koschny, E. N. Economou, and C. M. Soukoulis, Phys. Rev. Lett. **102**, 053901 (2009).
 - ²¹ P. Tassin, L. Zhang, T. Koschny, E. N. Economou, and C. M. Soukoulis, Opt. Express **17**, 5595 (2009).
 - ²² N. Liu, L. Langguth, T. Weiss, J. Kästel, M. Fleischhauer, T. Pfau, and H. Giessen, Nature Mater. **8**, 758 (2009).
 - ²³ V. Yannopapas, E. Paspalakis, and N. V. Vitanov, Phys. Rev. B **80**, 035104 (2009).
 - ²⁴ S.-Y. Chiam, R. Singh, C. Rockstuhl, F. Lederer, W. Zhang, and A. A. Bettiol, Phys. Rev. B **80**, 153103 (2009).
 - ²⁵ R. W. Ziolkowski, IEEE Trans. Antennas Propag. **51**, 1516 (2003).
 - ²⁶ V. A. Fedotov, M. Rose, S. L. Prosvirnin, N. Papasimakis, and N. I. Zheludev, Phys. Rev. Lett. **99**, 147401 (2007).
 - ²⁷ C. L. Garrido Alzar, M. A. G. Martinez, and P. Nussenzeig, Am. J. Phys. **70**, 37 (2002).
 - ²⁸ I. Gil, J. García-García, J. Bonache, F. Martín, M. Sorolla, and R. Marqués, Electron. Lett. **40**, 1347 (2004).
 - ²⁹ R. E. Collin, *Field Theory of Guided Waves* (IEEE Press, Piscataway, NJ, 1990), 2nd ed.
 - ³⁰ D. R. Smith, S. Schultz, P. Markoš, and C. M. Soukoulis, Phys. Rev. B **65**, 195104 (2002).
 - ³¹ H.-T. Chen, J. F. O'Hara, A. K. Azad, A. J. Taylor, R. D. Averitt, D. B. Shrekenhamer, and W. J. Padilla, Nature Photon. **2**, 295 (2008).
 - ³² S. Xiao, U. K. Chettiar, A. V. Kildishev, V. Drachev, I. C. Khoo, and V. M. Shalaev, Appl. Phys. Lett. **95**, 033115 (2009).
 - ³³ M. J. Dicken, K. Aydin, I. M. Pryce, L. A. Sweatlock, E. M. Boyd, S. Walavalkar, J. Ma, and H. A. Atwater, Opt. Express **17**, 18330 (2009).
 - ³⁴ W. J. Padilla, A. J. Taylor, C. Highstrete, M. Lee, and R. D. Averitt, Phys. Rev. Lett. **96**, 107401 (2006).
 - ³⁵ H.-T. Chen, W. J. Padilla, J. M. O. Zide, A. C. Gossard, A. J. Taylor, and R. D. Averitt, Nature **444**, 597 (2006).